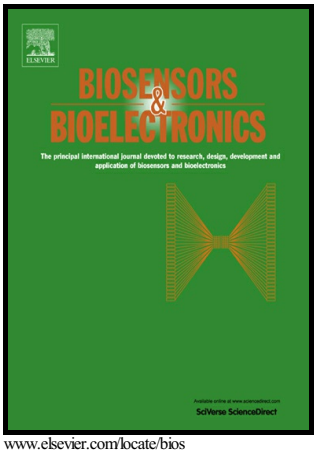

www.elsevier.com/locate/bios

A Nonenzymatic DNA Nanomachine for Biomolecular Detection by Target Recycling of Hairpin DNA Cascade Amplification

Jiao Zheng, Ningxing Li, Chunrong Li, Xinxin Wang, Yucheng Liu, Guobin Mao, Xinghu Ji, Zhike He

PII: S0956-5663(18)30066-6
DOI: https://doi.org/10.1016/j.bios.2018.01.054
Reference: BIOS10247

To appear in: *Biosensors and Bioelectronic*

Received date: 26 November 2017
Revised date: 22 January 2018
Accepted date: 24 January 2018

Cite this article as: Jiao Zheng, Ningxing Li, Chunrong Li, Xinxin Wang, Yucheng Liu, Guobin Mao, Xinghu Ji and Zhike He, A Nonenzymatic DNA Nanomachine for Biomolecular Detection by Target Recycling of Hairpin DNA Cascade Amplification, *Biosensors and Bioelectronic,* https://doi.org/10.1016/j.bios.2018.01.054

A Nonenzymatic DNA Nanomachine for Biomolecular Detection by Target Recycling of Hairpin DNA Cascade Amplification

Jiao Zheng, Ningxing Li, Chunrong Li, Xinxin Wang, Yucheng Liu, Guobin Mao, Xinghu Ji, Zhike He*

Key Laboratory of Analytical Chemistry for Biology and Medicine (Ministry of Education), College of Chemistry and Molecular Sciences, Wuhan University, Wuhan 430072, China

Abstract

Synthetic enzyme-free DNA nanomachine performs quasi-mechanical movements in response to external intervention, suggesting the promise of constructing sensitive and specific biosensors. Herein, a smart DNA nanomachine biosensor for biomolecule (such as nucleic acid, thrombin and adenosine) detection is developed by target-assisted enzyme-free hairpin DNA cascade amplifier. The whole DNA nanomachine system is constructed on gold nanoparticle which decorated with hundreds of locked hairpin substrate strands serving as DNA tracks, and the DNA nanomachine could be activated by target molecule toehold-mediated exchange on gold nanoparticle surface, resulted in the fluorescence recovery of fluorophore. The process is repeated so that each copy of the target can open multiplex fluorophore-labeled hairpin substrate strands, resulted in amplification of the fluorescence signal. Compared with the conventional biosensors of catalytic hairpin assembly (CHA) without substrate in solution, the DNA nanomachine could generate 2 to 3 orders of magnitude higher fluorescence signal. Furthermore, the DNA nanomachine could be used for nucleic acid, thrombin and adenosine highly sensitive specific detection based on isothermal, and homogeneous hairpin DNA cascade signal amplification in both buffer and a complicated biomatrix, and this kind of DNA nanomachine could be efficiently applied in the field of biomedical analysis.

Keywords: biomolecule detection, DNA nanomachine, fluorescence, gold nanoparticles, hairpin DNA cascade amplification.

1.Introduction

Molecular machines perform diverse biological functions in living systems (He et al., 2016; Li et al., 2016; Peng et al., 2017; Chen et al., 2016). In particular, DNA self-assembly represents a highly programmable approach to construct nanoscale molecular machines which can convert chemical energy to mechanical motions (Cha et al., 2014; Jiang et al., 2013). Biological or synthetic DNA nanomachines assembled with molecular components, which could be powered by DNAzymes (Peng et al., 2017), protein enzymes and strand displacement (Jung et al., 2016; Qu et al., 2017; Yang et al., 2016), and perform quasi-mechanical movements in response to specific external stimuli (Zhang et al., 2015). Extensive attention has been focused on designing artificial molecular machines but a challenge in engineering molecular machines is to improve the detection sensitivity of the nanomachines in a nanoscale objective along a designated path (Liu et al., 2014; Tian et al., 2005). Many exquisite specificity, predictability and diversity of DNA nanomachines have been constructed (Bi et al., 2014; Yao et al., 2016) based on the well defined Watson-Crick base pairing rule (Szymanski et al., 2017), including DNA walkers (Cha et al., 2014; Sherman and Seeman 2004; You et al., 2012), DNA tweezers (Yurke et al., 2000; Zhou et al., 2012) and DNA robots (Amir et al., 2014; Lund et al., 2010). Recently, well-defined three-dimensional (3D) DNA nanomachine has been reported and target recycling amplification strategy has attracted increasing interest in highly sensitive detection of biomolecules, then DNA self-assembly represents a highly programmable approach to construct molecular machines. For example, Li and co-walkers have recently described an enzyme-powered 3D DNA nanomachine for DNA nanomachine biosensor (Yang et al., 2016). The activity of the 3D DNA nanomachine can be controlled by introducing a protecting DNA probe and the efficiency is very high, but the movement of the DNA walker is powered by a nicking endonuclease.

Many published DNA nanomachines which used DNAzymes (Peng et al., 2017), protein enzymes (Wickham et al., 2011) or a chemical fuel such as Hg^{2+}/cysteine (Wang et al., 2011) to drive the movement of the walker for biomolecular detection. To avoid tedious procedure, and enzyme degrading under unfavorable environmental conditions. An enzyme-free DNA nanomachine was constructed potentially by using a gold nanoparticles (AuNP) substrate rather than a confined one-dimensional or two-dimensional track (Wickham et al., 2011; Yang et al., 2016). Hairpin DNA cascade

amplification (Yin et al., 2008) as an enzyme-free signal amplification strategy was introduced on AuNP surface to improve the detection sensitivity of the nanomachine biosensor and open up a new approach for a DNA nanomachine to merge with biosensor (Figure 1). In the previous hairpin DNA cascade amplification strategy, with single-stranded catalyst (S-catalyst), two kinetically trapped hairpins can undergo strand exchange reactions, resulting in the formation of a double-stranded nucleic acid and recycling of the S-catalyst. In traditional hairpin DNA cascade amplification experiment, the S-catalyst appeared to diffuse away without significant rebinding. There was also a global loss rate that accounts for a catalyst that may be released to the solution (as showed in Figure S1. The nanomachine could be driven only by a higher concentration of S-catalyst). To meet this challenge, we developed a DNA nanomachine which driven by double feet catalyst (D-catalyst) to improve the operation efficiency of DNA nanomachine. In greater detail, the D-catalyst was simple but elegant in design, which was a longer single-stranded DNA oligonucleotide contained two catalyst domains separated by a linker (as showed in table S1), non-hybridizing spacer sequence. Besides, the D-catalyst took place of the S-catalyst to prevent itself from being released into the solution, which was confirmed by the comparison of detection sensitivity of this strategy with the previous (Jiang et al., 2013).

To test the universality of the proposed strategy, a DNA nanomachine that triggered by thrombin (or adenosine) was also designed for highly sensitive and specific detection of thrombin (or adenosine). The aptamer beacon is a hairpin-shaped DNA strand, modified at its 5' and 3' ends with a sulfydryl and a fluorophore respectively. After the hairpin-shaped DNA conjugated to the AuNPs, the self-complementary stem of aptamer beacon brought the close proximity of the fluorophore to the AuNPs, resulting in fluorescence quenching. Upon the interaction of aptamer with the thrombin (or adenosine), the hairpin structure was open then the nanomachine was triggered, leading to the specific detection of thrombin (or adenosine) based on fluorescence restoration. In a word, we set the stage for sensitive detection of various targets, including nucleic acid, protein and small molecule which are extremely important in disease diagnosis.

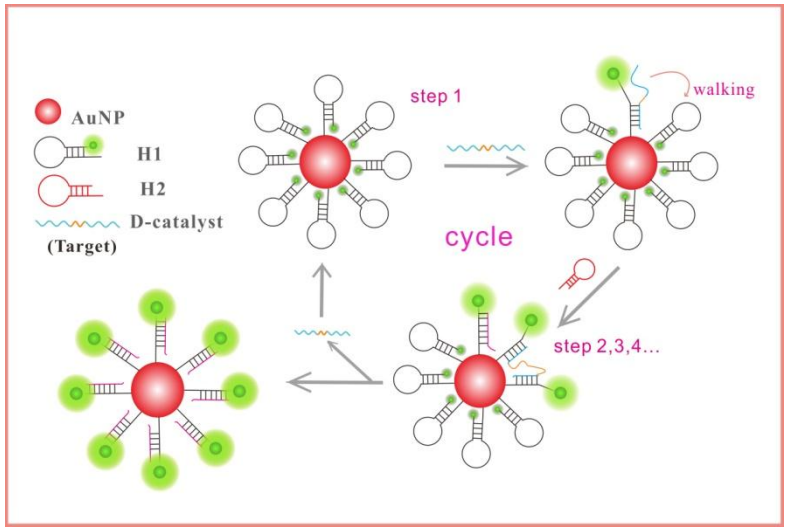

Figure 1. Schematic for nanomachine on gold nanoparticles surface triggered by D-catalyst and shows how some H2 are catalytically hybridized to the surface immobilized H1.

2. Materials and methods

2.1 Materials and instruments

Solution of gold nanoparticles (28.5 nm in average diameter) was synthesized as previously reported. (Haiss et al., 2007) Tris(hydroxy-methyl) aminomethane hydrochloride (Tris), magnesium chloride hexahydrate ($MgCl_2{\cdot}6H_2O$), sodium chloride (NaCl), potassium chloride (KCl), dithiothreitol (DTT), adenosine, thrombin, BSA and ATP, lysozyme, trypsin, guanosine and cytidine were purchased from Sigma-Aldrich (USA). All of the other reagents were of analytical-reagent grade or better. All pure water with a resistivity of 18.2 MΩ cm was purified by Milli-Q Academic purification set from Millipore.

All oligonucleotides with different sequences were synthesized and HPLC purified by Sangon Biotechnology Co., Ltd (Shanghai, China). The sequences of the oligonucleotide used in this work are as table S1.

Fluorescence spectra were recorded with a RF-5301PC spectrophotometer (Shimadzu, Japan) equipped with a 150 W xenon lamp (Ushio Inc, Japan), and the fluorescence emission intensity was measured at 518 nm with an excitation wavelength of 480 nm. Gels were imaged by a ChemiDoc XRD system (Bio-Rad). Transmission electron microscopy (TEM) and high-resolution (HR) TEM images were recorded on a JEOL Ltd. JEM 2100 electron microscope (Japan). X-ray photoelectron spectroscopy (XPS) characterizations of Au-H1 were recorded using an ESCA Lab electron

spectrometer (Thermal Fisher Scientific).

2.2 The synthesis of gold nanoparticle and preparation of polyvalent oligonucleotides gold nanoparticle conjugates

28.5 nm gold nanoparticle solution was synthesis as previously reported (Haiss et al., 2007). In brief, the vigorously stirred solution (125 mL, 254 μM $HAuCl_4 \cdot 3H_2O$) was brought to boiling in a silicone oil bath (at 125-150 °C). Rapid addition of 12.5 mL of 40 mM sodium citrate to the stirred $HAuCl_4$ solution resulted in a color change from pale yellow to dark red. The color change occurred over several minutes. The solution was kept for 10 minutes at boiling temperature and then removed from the heating kettle. Stirring was expected to continue for another 15 min, then the solution cooled to room temperature. Thus prepared AuNPs were stored at 4 °C.

A volume of 19 μL of thiol-modified oligonucleotides (100 μM) was mixed with 4.4 mL of AuNP solution and then stirred overnight at room temperature. After incubation for 16 hours, the mixture were diluted with phosphate buffer (0.15 M NaCl, pH 7.4) for five times at 30 minutes interval, then over an 40 hours period to achieve a final concentration of phosphate and NaCl was 10 mM and 0.1 M, respectively. The particles were washed from dissociative oligonucleotides by three successive rounds of centrifugation (15,000 rcf, 20 min), and the particles were resuspended in phosphate buffered saline (PBS) (100 mM NaCl, 10 mM phosphate, pH 7.4) and stored at 4 °C.

2.3 The quantification of hairpin substrate strands modified on gold nanoparticle surface

On the basis of the previously method, the hairpin substrate strands on the surface of AuNPs were calculated (Yang et al., 2016). The coverage of H1 on each AuNP was then determined by measuring fluorescence of the FAM (5-carboxyfluorescein) dye that was labeled on H1. Dithiothreitol (DTT) was added (final concentration was 20 mM) to the hairpin substrate strand conjugated AuNP solution and incubated overnight with gently shaking at room temperature. After that, the gold aggregation was separated and collected by centrifugation and the fluorescence of supernatant was measured with a fluorescence spectrometer.

2.4 Agarose gel electrophoresis of hairpin DNA cascade amplification

In a typical procedure, the hairpin DNA was diluted with 20 mM Tris-HCl buffer (140 mM NaCl, 5 mM KCl, pH = 7.4) and denatured at 95 °C for 5 minutes followed with a slow annealing treatment to room temperature. The gel electrophoresis were registered by adding 5 μL of different DNA solution (final concentration was 10 μM) in the mixture of loading buffer and 3.0 μL of bromophenol blue, respectively. The mixture was stained with 100 × SYBR Green I (1 μL), and marker DNA solution (100 μM) as indicators. 3 % agarose gel was prepared by using 1× TAE buffer (40 mM Tris AcOH, 2 mM Na_2EDTA, pH 8.5). The electrophoresis was carried out at 100 V for approximately 40 min in 1× TAE buffer. Then the gel was imaged by a ChemiDoc XRD system (Bio-Rad).

2.5 In vitro detection of target (nucleic acid, thrombin and adenosine)

The performance of the DNA nanomachine responding to D-catalyst was investigated by the fluorescence intensity of the dye recovered from AuNPs surface. Unless otherwise stated, sample solutions contained 30 μL DNA-functionalized AuNPs, 50 nM H2, different concentrations of D-catalyst in 20 mM Tris-HCl (pH 7.4) buffer containing 140 mM NaCl, 5 mM KCl. After that, the stock solution of catalyzed hairpin assembly reactions was incubated for 3 hours at 37 °C. The fluorescence intensity was measured by using 480 nm for excitation and 518 nm for emission wavelength, respectively.

To test the universality of the proposed method, we constructed a DNA nanomachine that triggered by thrombin. The different amounts of thrombin were mixed with functionalized AuNPs, 50 nM H2 of thrombin in 20 mM Tris-HCl (140 mM NaCl, 5 mM KCl, pH 7.4) solution and the final volume was 300 μL. After incubation at 37 °C for 3 hours, the fluorescence intensity was measured.

Then the efficiency of the nanomachine powered by adenosine was tested. The study of the performance of the nanomachine for adenosine was comparable to that for nucleic acid (D-catalyst). Adenosine was used as input, after adenosine was first incubated with aptamer-input (A-3)/inhibitor (A-4) for 1 h at 37 °C in 20 mM Tris-HCl (pH 7.4) solution. Then, 30 μL functionalized AuNPs, 50 nM (A-2), and various concentrations of adenosine/aptamer complex were mixed in the total volume of 300 μL of the same buffer solution. Fluorescence intensities were tested after incubating for 3 h at 37 °C.

3.Results and discussion

3.1 Construction and characterization of the 3D nanomachine

Many DNA nanomachines are powered by strand displacement, then we attempt to perform a feasibility test to determine whether the hairpin DNA cascade amplification could proceed on nanoparticle surfaces. As illustrated in Figure 1, we designed a 3D DNA nanomachine by conjugating FAM-labeled hairpin DNA substrates (H1), as a signal reporter, to AuNPs surface. Firstly, the fluorescence of FAM (5-carboxyfluorescein) on H1 was quenched. Once DNA nanomachine powered by the D-catalyst, the hairpin DNA substrate was opened, resulted in liberating the FAM-labeled DNA payload and turning on the fluorescence. Secondly, a newly exposed ssDNA region within the H1 then hybridize to a toehold on H2 and trigger branch migration, ultimately forming the most thermodynamically favourable configuration, the H1-H2 duplex. With displacement of the D-catalyst, which lead to the D-catalyst foot of the locality “walk” onto neighboring hairpin DNA substrate and participate in subsequent reaction cycles. And the D-catalyst as a dynamite fuse, a strong fluorescence can be ignited. More importantly, this strategy can be employed to the detection of nucleic acid, protein and small molecule.

3.2 Feasibility investigation and the concentration of H1 modified on gold nanoparticle surface

The feasibility of the proposed nanomachine biosensor was measured by fluorescence spectrometer. In Figure 2A, the fluorescence intensity of the proposed biosensor was presented in the absence and presence of D-catalyst (target), respectively. In the absence of target, a low fluorescence signal was obtained (curve b). However, a significant fluorescence signal appeared (curve d) in the presence of target (370 pM), indicating the successful operation in DNA nanomachine as well as the feasible construction of the biosensor for nucleic acid determination. For comparison, we have studied the release of fluorophores on the surface of nanoparticle with absence of H2 (curve c). In the absence of H2, D-catalyst was linear hybridization probe, target signaling occurred in an equivalent reaction ratio (1:1) and the D-catalyst can't walk to the next round, resulting in low sensitivity. Proven that H2 could exchange D-catalyst and form duplex reaction product which would resolve into the most

thermodynamically favorable configuration, the H1-H2 duplex and target is able to yield multiple signal outputs (1:m). With displacement of the walking D-catalyst which could generate a 2 to 3 orders of magnitude higher fluorescence signal than that of no amplification experiments.

Next, agarose gel electrophoresis (3%) was further applied to verify the feasibility of hairpin DNA cascade amplification reaction triggered by S-catalyst or D-catalyst. As outlined in Figure 2B, due to stem-and-loop of H1 and H2 no obvious band was obtained in lane 1 and 2. In lane 3 and 4, S-catalyst (or D-catalyst) was a single strand so that exhibited a blank band. In lane 7 and 10, S-catalyst (or D-catalyst) couldn't hybridize with H2 resulted in weak band. In lane 5, due to high concentration of H1 and H2, a light band was observed. The binding of H1 and H2 seems thermodynamically stable (27 bonds were broken and 35 bonds were newly created), but two hairpins are kinetically trapped, only in the presence of S-catalyst (or D-catalyst) can undergo strand exchange reactions that lead to the formation of a double-stranded nucleic acid and recycling of the S-catalyst (or D-catalyst). In lane 6 and 8, due to S-catalyst could combine with H1 then form H1-S-catalyst, light band of the same migration rate was observed. Lane 8 also produce a weak band of H1-H2 complex. In lane 6 and 9, just because of D-catalyst has two same S-catalyst domains which could combine with two H1 then the band of lane 9 with slower mobility. In lane 11, two bands in lane 11 indicates that H1-D-catalyst-H1 and H1-H2 were produced. The band of lane 8 was lighter than lane 11, because of the hairpin DNA cascade amplification reaction without AuNPs, and the length of S-catalyst was shorter than D-catalyst, resulted in S-catalyst would appeal to release and diffuse under strand exchange reactions in high concentration of reactants. The above results successfully confirmed that the proposed method was entirely feasible for nucleic acid detection.

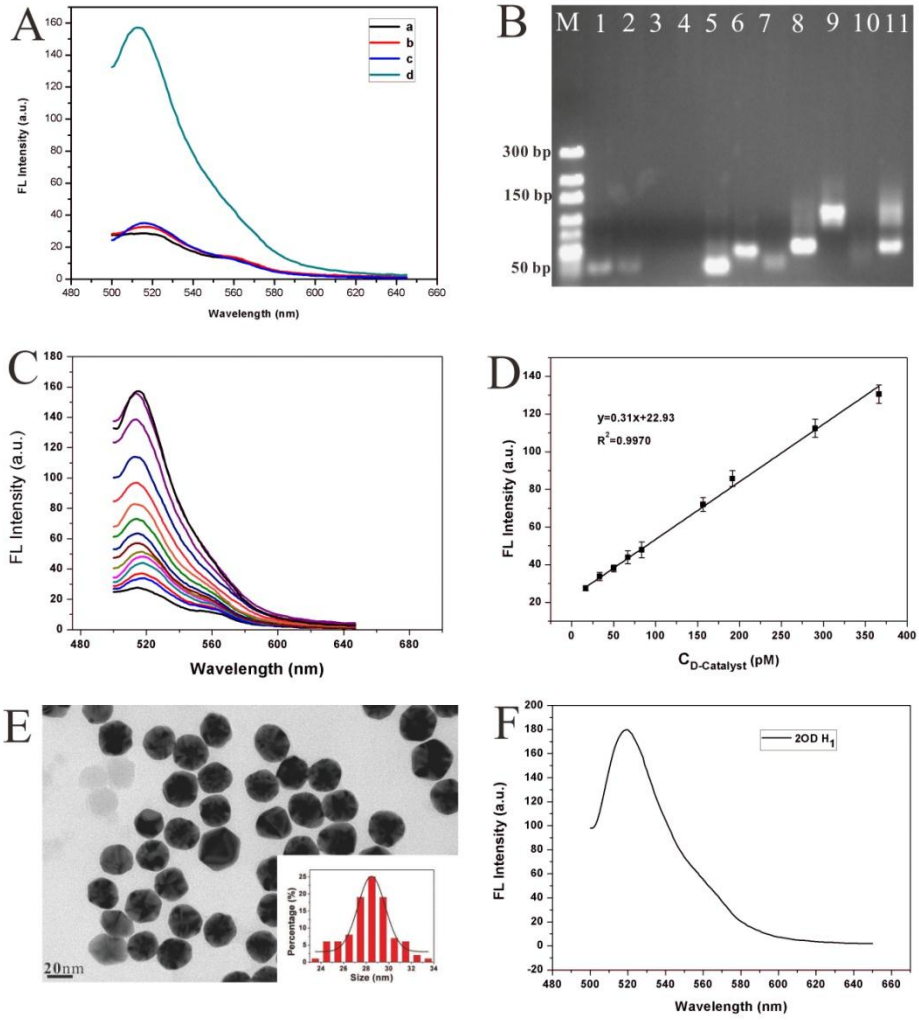

Figure 2. (A) Fluorescence spectra of the system under different conditions: (a) AuNPs-H1; (b) AuNPs-H1 in the presence of H2 (66.67 nM) and without D-catalyst; (c) AuNPs-H1 in the presence of D-catalyst (370 pM) and without H2; (d) AuNPs-H1 in the presence of D-catalyst (370 pM) and H2 (66.67 nM). (B) 3% agarose gel electrophoresis of the products of different experiments. Lane M: DNA ladder; lane 1: H1; lane 2: H2; lane 3: S-catalyst; lane 4: D-catalyst; lane 5: H1+H2; lane 6: H1+S-catalyst; lane 7: H2+S-catalyst; lane 8: H1+H2+S-catalyst; lane 9: H1+D-catalyst; lane 10: H2+D-catalyst; lane 11: H1+H2+D-catalyst. And the concentrations were all 10 μM. (C) Fluorescence spectra of various concentration of H1-FAM. (D) Standard curve of H1. (E) TEM images of the synthesis of AuNPs. The inset is the size distribution of AuNPs. (F) Fluorescence spectra of H1 that modified on gold nanoparticles by dealing with DTT.

3.3 Optimization of the nanomachine reaction conditions

The labeled H1 were assembled on the surface of AuNPs by the Au–S bond. The morphology of the AuNPs was characterized by TEM (Figure 2E). And morphology of AuNPs functionalized with H1 was characterized by cryo TEM, XPS as well (Figure S2). The images showed that the border of the AuNPs was clear and that of the nanoprobe was obscured, suggesting the successful assembly of H1 on the surface of

AuNPs. The coverage of H1 on each AuNP was determined, and we also calculated the average concentration of AuNP based on the atomic absorption spectrum and the diameter of the gold nanoparticles. As showed in Figure 2F, the concentrations of FAM-labeled DNA were determined by interpolation fluorescence signal from a standard linear calibration curve (Figure 2C, D) that was prepared with known concentrations of oligonucleotide with identical buffer and DTT concentration. The results showed the concentration of H1 modified on gold nanoparticles was 23.2 nM. According to the previously reported method (Yang et al., 2016), the average concentration of AuNP and the coverage of H1 on each AuNP were determined (Figure S3). The result was approximately 127 strands of H1 per AuNP. And the average number of walking steps is 20.

The optimal operation condition of constructed DNA nanomachine was studied to meet the goal of efficient payload release, and each component can potentially have a influence on its overall efficiency. To better understand the effect of some components for DNA nanomachine operation, we have investigated the effect of various experimental conditions including ion strength, the length of D-catalyst and the reaction time. As showed in Figure S4, 5, with the ion strength and the length of D-catalyst varied, the fluorescence changed slightly. According to an investigation of the limited influence, the reaction condition (20 mM Tris-HCl, 5 mM KCl, 140 mM NaCl, pH 7.4) and 76 bases D-catalyst were chosen in the next investigation. On the other hand, the reaction time of DNA nanomachine was investigated toward efficient payload release. Figure 3A revealed the fluorescence signals corresponding to different time periods. The fluorescence intensity of FAM was very slight at first and then increased gradually before reaching a platform. 3 h was selected as the optimum reaction time of DNA nanomachine.

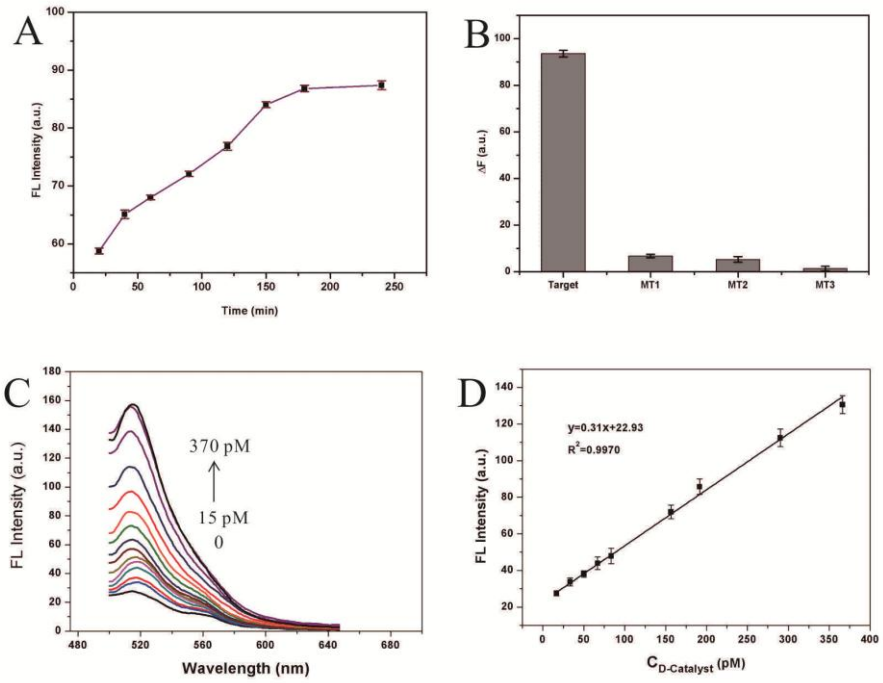

Figure 3. (A) Monitoring the fluorescence increases of H1-AuNP as a relationship of time. (B) Relative fluorescence response from different inputs of same concentration. (C) Fluorescence spectra of the strategy to convert a 3D DNA nanomachine into a DNA nanosensor. (D) Relationship between the fluorescence intensity and D-catalyst concentration and calibration curve for D-catalyst detection.

3.4 DNA nanomachine biosensor triggered by nucleic acid

Under the optimized conditions, the analytical performance of the present biosensor is investigated by using various concentrations of target (D-catalyst). As showed in Figure 3C, D the fluorescence intensity steadily increases with the concentration of target from 15 pM to 370 pM, suggesting that the DNA machine for the fluorescence signal readout is highly dependent on the concentration of target nucleic acid. The linear regression equation can be expressed as follows: F (a.u.)= $0.31C_{target}$+ 22.93 with a correlation coefficient of 0.9970. Additionally, the detection limit of the present biosensor for target nucleic acid is estimated to be as low as 3.4 pM according to $3S_B$ /m in which the S_B is the standard deviation of the blank sample (n=11) and m is the slope of the obtained equation, which is superior to those of the previously reported biosensors based on the amplification strategies (Table 1). These results indirectly reveal the high amplification efficiency of hairpin DNA cascade amplification.

The selectivity of the proposed nanomachie biosensor is further investigated by using four DNA sequences, including the target, the single-base mismatched target (MT1), the two-base mismatched target (MT2), and the three-base mismatched target

(MT3) at the same concentration, and the results are shown in Figure 3B. These observations demonstrate that the designed DNA nanomachine biosensor could effectively discriminate different nucleic acid and display an excellent selectivity for nucleic acid assay.

To demonstrate the practical applications and analytical reliability of the designed DNA nanomachine biosensor, D-catalyst in real serum samples are assayed as outlined above. Subsequently, different concentrations of D-catalyst are spiked into the serum samples and detected by the same procedure. Table 1 demonstrates favorable spiking recoveries for D-catalyst at various concentration levels. These results clearly indicate the favorable accuracy of the designed biosensor for the detection of nucleic acid in real biological samples.

Table 1 Recovery of nucleic acid in bovine serum with this proposed method.

Sample number	**Added (pM)**	**Found (pM)**	**Recovery (%)**	**RSD (%) (n = 3)**
1	30	29.35± 0.53	97.8	1.8
2	60	60.73±2.4	101.2	4.0
3	100	99.18±1.3	99.2	1.3
4	150	151.2±3.4	100.8	2.2
5	200	208.1±6.2	104.1	3.0

3.5 Engineering DNA nanomachine biosensor triggered by any other biomolecules

We further investigated the use of thrombin or adenosine as a driving motor to trigger the DNA nanomachine. As showed in Figure 4A, taken thrombin as the model analyst, AuNPs was conjugated with T-H1 which contains two domains. Domain one is an aptamer (labeled of FAM) of thrombin which is blocked by hybridization with the rest domain, then the fluorescence of the fluorophore was quenched by gold nanoparticles. The region of T-H2 is complementary with the part of T-H1 and is blocked by hybridization with the rest region. In the absence of thrombin, these two hairpins T-H1 and T-H2 interact barely with each other. In the presence of thrombin, the opening of the hairpin structure of T-H1 is facilitated, making it accessible for hybridization with T-H2. Then, the thrombin can be displaced from hairpin T-H1 by hairpin T-H2 through a process similar to DNA branch migration. The released thrombin can walk to another

T-H1, and the cycle starts anew. In this way, a single thrombin can generate many T-H1-T-H2 complexes, which lead to the significant fluorescence restoring. The linear regression equation can be expressed as follows: F (a.u.)= 189.01C_{target}+ 31.11 with a correlation coefficient of 0.9984 (Figure 4C). Additionally, the detection limit of the present biosensor for thrombin is estimated to be as low as 57 pM according to $3S_B$ /m in which the S_B is the standard deviation of the blank sample (n=11) and m is the slope of the obtained equation. By monitoring the change in fluorescence intensity, the thrombin could be detected with higher sensitivity (Table 2). The selectivity of the proposed nanomachie biosensor is further investigated by using BSA, lysozyme, trypsin, thrombin at the same concentration, and the results are shown in Figure 4E. These observations demonstrate that the designed DNA nanomachine biosensor could effectively discriminate different protein and display an excellent selectivity for thrombin assay.

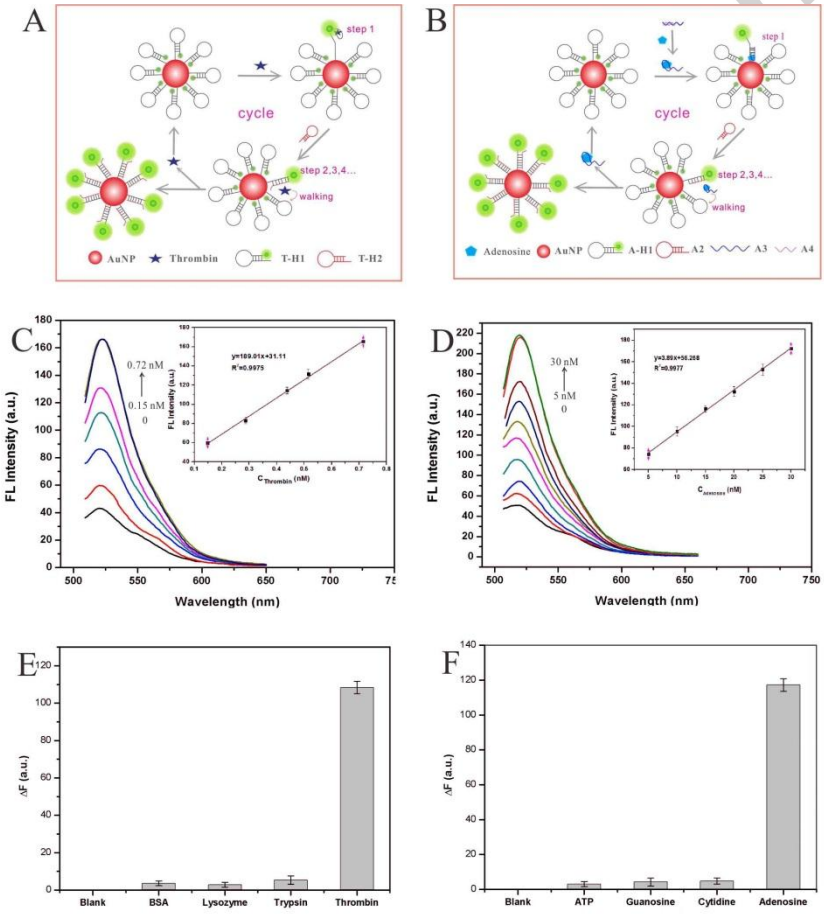

Figure 4. (A) Schematic of the nanomachine responsive to thrombin. (B) Schematic of the nanomachine responsive to the small molecular adenosine. (C) Fluorescence responses of the present biosensor to different concentrations of thrombin. Inset: the linear relationship of the peak fluorescence intensity versus thrombin concentration. (D) Fluorescence responses of the present biosensor to different concentrations of adenosine. Inset: the linear

relationship of the peak fluorescence intensity versus adenosine concentration. (E) Selectivity test for the present biosensor for thrombin assay. (F) Selectivity test for the present biosensor for adenosine assay.

We also took advantage of the analogous principle for the detection of adenosine. As showed in Figure 4B, we designed structure-switching aptamer that exposed a toehold in response to adenosine. Adenosine reacts with duplex (A3-A4), which contains catalyst domain and aptamer hybridized with a piece of ssDNA (inhibitor). This ssDNA converted adenosine input to DNA for the following cascade reactions. The catalyst domain with adenosine then walked to the next assembly module, ultimately produced a strongly fluorescence signal. The linear regression equation can be expressed as follows: F (a.u.)= $3.89C_{target}$+ 56.268 with a correlation coefficient of 0.997 (Figure 4D). Additionally, the detection limit of the present biosensor for thrombin is estimated to be as low as 1.22 nM according to $3S_B$ /m in which the S_B is the standard deviation of the blank sample (n=11) and m is the slope of the obtained equation. This is lower than that of most of the previously reported amplification aptasensors for adenosine detection (Table 1). The selectivity of the proposed nanomachie biosensor is further investigated by using ATP, guanosine, cytidine, adenosine at the same concentration, and the results are shown in Figure 4F. These observations demonstrate that the designed DNA nanomachine biosensor could effectively discriminate different target molecule and display an excellent selectivity for adenosine assay.

Table 2. Comparison of the reported chemosensors for nucleic acid, thrombin and adenosine.

Target detection	No.	Detection method	Dynamic range	Limit of detection	Ref.
For nucleic acid detection	1	Electrochemical assay	0-5 nM	0.33 nM	(Laschi et al., 2010)
	2	Fluorescence detection	2.5-25 nM	1.8 nM	(Yan et al., 2015)
	3	Fluorescence detection	not mentioned	20 nM	(Yang et al., 2016)
	4	Flow cytometry	not mentioned	5 nM	(Jung et al., 2016)
	5	This method	15-370 pM	3.44 pM	
For thrombin detection	1	Liquid chromatography/tandem mass spectrometry	0.5-50 nM	0.30 nM	(Du et al., 2014)
	2	Localized surface plasmon resonance	0-0.19 mM	12.0 nM	(Jalit et al., 2013)
	3	Electrochemiluminescence detection	0-20 mg/mL	not mentioned	(Huang and Zhu 2009)
	4	Fluorescence detection	0-500 nM	1.1 nM	(Kong et al., 2013)
	5	Colorimetric detection	0-2 nM	0.05 nM	(Na et al., 2015)
	6	This method	0.15-0.72 nM	57 pM	
For adenosine	1	Fluorescence detection	1-120 μM	0.2 μM	(Feng et al., 2016)

detection					
	2	Localized surface plasmon resonance	5-500 nM	5 nM	(Xu et al., 2015)
	3	Fluorescence detection	1-100 μM	0.42 μM	(Sun et al., 2015)
	4	Fluorescence detection	1-8 mM	0.3 mM	(Lin and Tseng 2013)
	5	Dynamic light scattering	8-80 nM	7 nM	(Yang et al., 2011)
	6	This method	5-30 nM	1.23 nM	

4. Conclusion

In conclusion, we designed a DNA nanomachine based on hairpin DNA cascade amplification on nanoparticle surface. In this proposed strategy, chain hybridization replaces enzyme to drive walking on DNA-coated nanoparticles surface, having the advantage of simple, low-cost, sufficiently sensitive and higher versatility. Besides, gold nanoparticles played several important roles in this strategy. First, gold nanoparticles, as a platform, constructed a three-dimensional DNA−AuNP track which made the operation locally ordered on nanoparticle surface; second, the corresponding increases in local effective concentrations of H1 on AuNP surface also accelerated the catalytic efficiency; furthermore, gold nanoparticles could be a quencher to quench the fluorophore before nanomachine operation. In the end, we are succeeding in designing an enzyme-free DNA nanomachine and subsequent opening up new concepts and strategies in dynamic DNA nanotechnology, which may advance the application of new DNA nanomachine in biosensors.

Acknowledgements.

This work was supported by the National Natural Science Foundation of China (21675119, 21475101).

References.

Amir, Y., Ben-Ishay, E., Levner, D., Ittah, S., Abu-Horowitz, A., Bachelet, I., 2014. Nat Nanotechnol. 9 (5), 353-357.

Bi, S.; Cui, Y. Y.; Dong, Y.; Zhang, N. B., 2014. Biosens. Bioelectron. 53, 207-213.

Cha, T. G., Pan, J., Chen, H. R., Salgado, J., Li, X., Mao, C. D., Choi, J. H., 2014. Nat Nanotechnol. 9 (1), 39-43.

Chen, J. B., Deng, B., Wu, P., Li, F., Li, X. F., Le, X. C., Zhang, H. Q., Hou, X. D., 2016. Chem. Commun. 52 (9), 1816-1819.

Du, F., Alam, M. N., Pawliszyn, J., 2014. Anal. Chim. Acta 845, 45-52.

Feng, C. J., Hou, Z., Jiang, W., Sang, L. H., Wang, L., 2016. Biosens. Bioelectron. 86, 966-970.

Haiss, W., Thanh, N. T. K., Aveyard, J., Fernig, D. G., 2007. Anal. Chem. 79 (11), 4215-4221.

He, X. W., Zeng, T., Li, Z., Wang, G. L., Ma, N., 2016. Angew. Chem., Int. Ed. 128 (9), 3125-3128.

Huang, H. P., Zhu, J. J., 2009. Biosens. Bioelectron. 25 (4), 927-930.

Jiang, Y., Li, B., Milligan, J. N., Bhadra, S., Ellington, A. D., 2013. J. Am. Chem. Soc. 135 (20), 7430-7433.

Jalit, Y., Gutierrez, F. A., Dubacheva, G., Goyer, C., Coche-Guerente, L., Defrancq, E., Labbé, P., Rivas, G. A., Rodríguez, M, C., 2013. Biosens. Bioelectron. 41, 424-429.

Jung, C., Allen, P. B., Ellington, A. D., 2016. Nat Nanotechnol. 11 (2), 157-163.

Kong, L., Xu, J., Xu, Y. Y., Xiang, Y., Yuan, R., Chai, Y. Q., 2013. Biosens. Bioelectron. 42, 193-197.

Laschi, S., Miranda‐Castro, R., González‐Fernández, E., Palchetti, I., Reymond, F., Rossier, J. S., Marrazza, G., 2010. Electrophoresis 31 (22), 3727-3736.

Li, F., Cha, T. G., Pan, J., Ozcelikkale, A., Han, B., Choi, J. H., 2016. Chem. Bio. Chem. 17 (12), 1138-1141.

Lin, J. H., Tseng, W. L., 2013. Biosens. Bioelectron. 41, 379-385.

Liu, X. Q., Lu, C. H., Willner, I., 2014. Acc. Chem. Res. 47 (6), 1673-1680.

Lund, K., Manzo, A. J., Dabby, N., Michelotti, N., Johnson-Buck, A., Nangreave, J., Taylor, S., Pei, R. J., Stojanovic, M. N., Walter, N. G., Winfree, E., Yan, H., 2010. Nature 465 (7295), 206-210.

Na, W. D., Liu, X. T., Wang, L., Su, X. G., 2015. Anal. Chim. Acta 899, 85-90. Peng, H. Y., Li, X. F., Zhang, H. Q., Le, X. C., 2017. Nat. Commun 8, 14378.

Qu, X. M., Zhu, D., Yao, G. B., Su, S., Chao, J., Liu, H. J., Zuo, X. L., Wang, L. H., Shi, J. Y., Wang, L. H., Huang, W., Pei, H., Fan, C. H., 2017. Angew. Chem., Int. Ed., 56 (7), 1855-1858.Sherman, W. B., Seeman, N. C., 2004. Nano Lett. 4 (7), 1203-1207.

Sun, J. W., Jiang, W., Zhu, J., Li, W., Wang, L., 2015. Biosens. Bioelectron. 70, 15-20.

Szymanski, E. S., Kimsey, I. J., Al-Hashimi, H. M., 2017. J. Am. Chem. Soc. 139 (12), 4326-4329.

Tian, Y., He, Y., Chen, Y., Yin, P., Mao, C. D., 2005. Angew. Chem., Int. Ed. 44 (28), 4355-4358.

Wang, Z. G., Elbaz, J., Willner, Itamar., 2011. Nano Lett. 11 (1),304-309.

Wickham, S. F. J., Endo, M., Katsuda, Y., Hidaka, K., Bath, J., Sugiyama, H., Turberfield, A. J., 2011. Nat Nanotechnol. 6 (3), 166-169.

Xu, S. C., Man, B. Y., Jiang, S. Z., Wang, J. H., Wei, J., Xu, S. D., Liu, H. P., Gao, S. B., Liu, H. L., Li, Z. H., Li, H. S., Qiu, H. W., 2015. ACS Appl. Mater. Interfaces 7 (20), 10977-10987.

Yan, J. K., Ma, H. L., Cai, P. F., Wu, J. Y., 2015. Spectrochim. Acta. A Mol. Biomol. Spectrosc. 134, 17-21.

Yang, X. H., Huang, J. H., Wang, Q., Wang, K. M., Yang, L. J., Huo, X. Q., 2011. Anal. Methods 3 (1), 59-61.

Yang, X. L., Tang, Y. N., Mason, S. D., Chen, J., Li, F., 2016. ACS nano 10 (2), 2324-2330.

Yao, D. B., Li, H., Guo, Y. J., Zhou, X., Xiao, S. Y., Liang, H. J., 2016. Chem. Commun. 52 (48), 7556-7559.

Yin, P., Choi, H. M. T., Calvert, C. R., Pierce, N. A., 2008. Nature 451 (7176), 318-322.

You, M. X., Chen, Y., Zhang, X. B., Liu, H. P., Wang, R. W., Wang, K. L., Williams, K. R.; Tan, W. H., 2012. Angew. Chem., Int. Ed. 51 (10), 2457-2460.

Yurke, B., Turberfield, A. J., Mills, A. P., Simmel, F. C., Neumann, J. L., 2000. Nature 406 (6796), 605-608.

Zhang, H., Lai, M., Zuehlke, A., Peng, H., Li, X. F., Le, X. C., 2015. Angew. Chem., Int. Ed. 127 (48), 14534-14538.

Zhou, C., Yang, Z. Q., Liu, D. S., 2012. J. Am. Chem. Soc. 134 (3), 1416-1418.

Highlights

- Designed DNA nanomachines which can simultaneously fulfill local orderly operation and biosensor.
- AuNP as a carrier could improve effective concentrations of substrate strand (H1) and also accelerate the catalytic efficiency of target on nanoparticle surface.
- An enzyme-free amplification strategy was used for three biomolecules detection.
- Biosensors fabricated with DNA nanomachine have the advantage of simple, low-cost, sufficiently sensitive and higher versatility.